11. Seismic Properties of Leg 195 Serpentinites and Their Geophysical Implications[1]

Anna M. Courtier,[2, 3] David J. Hart,[4] and Nikolas I. Christensen[2]

ABSTRACT

Knowledge of seismic velocities is necessary to constrain the lithologies encountered in seismic studies. We measured the seismic velocities, both compressional and shear wave, of clasts recovered during Ocean Drilling Program Leg 195 from a serpentine mud volcano, the South Chamorro Seamount. The compressional wave velocities of these clasts vary from a lower value of 5.5 km/s to an upper value of 6.1 km/s at a confining stress of 200 MPa. The shear wave velocities vary from a lower value of 2.8 km/s to an upper value of 3.3 km/s at a confining stress of 200 MPa. The densities of the samples vary from 2548 to 2701 kg/m³. These velocities and densities are representative of the highly serpentinized harzburgite and dunite mineralogy of the clasts. Velocities from a seismic study of the Izu-Bonin forearc wedge were used to calculate the degree of serpentinization in the forearc wedge. The seismic velocities of the forearc wedge are higher than the velocities of the clasts recovered from the South Chamorro Seamount, suggesting that the clasts are more serpentinized than the forearc wedge.

INTRODUCTION

Serpentinite clasts were recovered from cores of serpentine mud from South Chamorro Seamount in the Mariana Trench region during Ocean Drilling Program (ODP) Leg 195. South Chamorro Seamount is one of many serpentine mud volcanoes located between the Mariana and Izu-Bonin forearc basins and the inner slope of the trenches. These serpen-

tine mud volcanoes form when water from the subducted Pacific plate interacts with the mantle rock in the subduction zone beneath the Philippine plate to form serpentinite. Because serpentinite is less dense than the surrounding mantle and ocean crust rocks, it will rise to the surface if a pathway is present. Faulting and seismicity in the forearc basins provide this pathway. The seismicity grinds the serpentinites into breccia that rises with excess fluids from the Benioff Zone to the surface through the forearc faults. This "mud" forms the serpentine mud volcanoes (Fryer et al., 2000). The clasts tested in this study were included in the serpentine mud. Similar to Ballotti et al. (1992), the purpose of this study is to examine the compressional and shear wave velocity and density ranges of clasts from the serpentine mud volcanoes. These data can then be used to estimate percent serpentinization of the mantle rock at depth if seismic velocities are available.

## STUDY CONDITIONS AND TECHNIQUE

In this study, velocities are reported for hydrostatic pressures up to 600 MPa at ambient temperature for 14 samples obtained from Leg 195 drilling. A core was taken from each sample using a 2.54-cm diameter diamond coring bit. Each core averages ~2 cm in length. The core ends were trimmed and ground flat and parallel to within 0.07 cm on a diamond grinding disk. The volume of each core was calculated from the length and diameter. The cores were weighed, and densities were calculated from their masses and dimensions. Each core was then fitted with a soldered copper jacket to prevent penetration of high-pressure oil into the rock samples. To make velocity measurements, 1-MHz transducers were affixed to both core ends. Gum rubber tubing was placed over the sample assembly as a further prevention of oil leakage.

Velocities were measured at room temperature and hydrostatic pressures up to 600 MPa using the pulse transmission method described by Christensen (1985). A pulse generator produced a 50-V square wave, simultaneously triggering a dual-trace oscilloscope. Readings were taken at 20, 40, 60, 80, 100, 150, 200, 250, 300, 350, 400, 450, 500, 550, and 600 MPa and repeated for downgoing pressures.

Interfacing the pressure system with a computer for data acquisition and storage permits automatic calculations of velocities as successive readings are taken. First break picks for acquired waveforms are automatically selected by the computer and can be fine-tuned by the operator. Using a least-squares routine, the computer fits a curve to the data points and calculates velocities for each pressure. A velocity vs. pressure curve is plotted along with recorded data points (Fig. F1). The sample length, density, measured pressure-velocity pairs, traces of the waveforms (Fig. F1) at selected pressures, the curve fit equations, and calculated pressure-velocity pairs are recorded and stored digitally.

Shipboard petrography of the rocks recovered from Site 1200 indicates that they are heavily serpentinized harzburgite and dunite clasts. (Shipboard Scientific Party, 2002). Minerals present include lizardite and chrysotile serpentine, olivine, orthopyroxene, Cr spinel, and trace amounts of clinopyroxene. In some cases the serpentinization obscures the original mineralogy. Some fracturing or cracking is also seen in the rocks.

F1. Confining pressure vs. compressional velocity, p. 7.
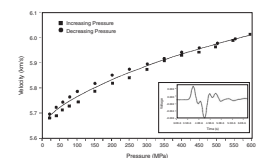
RESULTS

Compressional and shear wave velocity data at increasing pressures are presented in Table **T1.** V_P/V_S values and Poisson's ratios (*s*) calculated from these velocities at each pressure are presented in Table **T2.** Compressional wave velocities were measured for all 14 samples, and shear waves were measured for 8 samples. The estimated errors in the measurements are ±0.5% for compressional velocity, ±1% for shear velocity, and ±6% for Poisson's ratio (Christensen and Shaw, 1970). Although serpentinites may be anisotropic, it was not possible to prepare several samples from the core with different orientations because of the limited amount of rock. Therefore, it was not possible to determine seismic anisotropy of these samples from the velocity measurements. The anisotropy in serpentinites may be due to preferred alignment of relict olivine grains (Birch, 1961; Christensen, 1966), and values of Poisson's ratio may vary in excess of ±6% because the velocities were not measured in more than one direction. All of the rocks fall into a narrow density range between 2548 and 2701 kg/m³.

DISCUSSION

The mud volcanoes of the Mariana Trench region provide a unique look at rocks and fluids from a subduction zone. In this region, rock clasts and fluid-rich serpentine mud are brought from the forearc mantle wedge to the surface through faults in the overriding plate (Fryer, 1992, 1996). The densities and velocities of these rocks can be used in conjunction with seismic studies to constrain lithologies in subduction zones and the degree of alteration of the forearc mantle wedge.

Figure **F2** shows the average compressional velocity of the 14 samples measured as a function of confining pressure. These samples show relatively little increase in velocity with pressure, particularly at low pressures. Many rocks show a large initial rise in velocity at pressures below 100 MPa due to closing of grain-boundary microcracks in the rock (Birch, 1961). The slow rise in velocities in the Leg 195 serpentinites indicates a low microcrack content in these rocks. Shipboard velocity measurements were made on different Leg 195 clasts at ambient pressure (Shipboard Scientific Party, 2002). These compressional wave velocities ranged from 3.80 to 5.48 km/s and are significantly lower than compressional wave velocities measured in this study. The shipboard measurements are likely to have been more affected by porosity and microcracks in the samples rather than the mineralogy and structure of the clasts.

Christensen (1966) established a velocity-density relationship for partially serpentinized rocks. He found that both density and velocity decrease with increasing serpentinization. The data demonstrating these relationships at a pressure of 200 MPa are shown in Figure **F3**. Samples in the 1966 study included serpentinite, partially serpentinized peridotites, peridotites, and dunites, most of which were from Burro Mountain, California (USA). Rocks with a density of 2500 kg/m³ are nearly 100% serpentinized, and rocks with a density of ~3300 kg/m³ are fresh, unserpentinized peridotite and dunite. The Leg 195 samples measured at 200 MPa were compared to samples from Christensen (1966) and show a narrow range of both velocity and density (Fig. **F3**). All of the Leg 195 samples fall in the range of rocks measured by Christensen
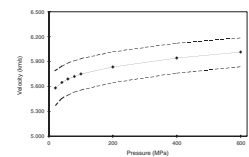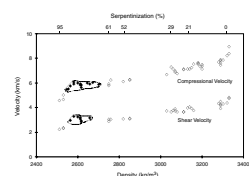
(1966) that are 61%–95% serpentinized. The low velocities and densities of these clasts, along with this observation, indicate that the Leg 195 clasts measured here are all highly serpentinized in agreement with petrographic observations. The Leg 195 data agree well with the 1966 data. For the limited range of velocity and density, the velocity-density trend defined in Christensen (1966) is seen in the Leg 195 samples as well. They have slightly higher velocities for their densities compared to the 1966 trend, which may be due to variations in accessory mineralogy or phase of the serpentine.

Compressional velocity vs. shear velocity for Leg 195 rocks at a pressure of 200 MPa is shown in Figure F4. A linear trend line $V_P = 0.757 V_S + 3.5375$ is plotted to fit the data. Considering the narrow range of velocities, the scatter about the line is low, with a regression coefficient of $r^2 = 0.81$. Dashed lines in the plot are lines of constant Poisson's ratio. Serpentinites characteristically have high Poisson's ratios (Christensen, 1996), and this is seen for these samples as well. Poisson's ratio increases with the degree of serpentinization, and is ~0.35 for 100% serpentine. As expected, samples with lower velocities, and therefore more serpentinization, have higher Poisson's ratios.

We used seismic studies of compressional wave velocities combined with knowledge of the geology of subduction zones to calculate the variation of serpentinization of the mantle rock in subduction zones. Assuming that the relationships from Christensen (1966) between velocity, density, and serpentinization apply at 200 MPa (~8 km depth), we can calculate percent serpentinization from a velocity. The percentage of serpentinite for the samples in Table T1 at a pressure of 200 MPa, corresponding to the mean velocity of 5.8 km/s using Christensen (1966), is ~66%. This values agrees reasonably well with the average degree of serpentinization of clasts (~70%) found by the Shipboard Scientific Party (2002).

For comparison, we calculated the percentage of serpentinite, assuming a lithostatic pressure of 200 MPa for the forearc mantle wedge, using velocities from a seismic study of the Izu-Bonin subduction zone (Kamimura et al., 2002). In that study, seismic surveys were conducted perpendicular to the Izu-Bonin Trench axis over a serpentine mud volcano, the Tori-shima serpentine forearc seamount, on a 130-km-long east-west line and parallel to the Izu-Bonin Trench axis on a 130-km-long north-south line. The Tori-shima mud volcano was studied during ODP Leg 125 and provided much of the data used to understand the South Chamorro serpentine mud volcano during Leg 195. Kamimura et al. (2002) identified nine layers in their east-west velocity model. Their Layer 6 corresponds to the forearc mantle wedge, the probable source of the muds for the serpentine mud volcanoes that line the Izu-Bonin and Marianna trench systems. In their velocity model of the forearc mantle wedge, the velocities decrease from 8.0 km/s at a distance of 162 km from the trench axis to 6.5 km/s at a distance of 62 km from the trench axis. This corresponds to an increase of percentage serpentinite from 4% at a distance of 162 km from the trench axis to 46% at a distance of 62 km from the trench axis. In a similar manner, the percentage of serpentinite in the layer corresponding to the forearc mantle wedge for the north-south seismic line of Kanimura et al. (2002) was also calculated. As noted in Kamimura et al. (2002), the area of lowest velocity on the north-south line in the forearc wedge is located nearest the Tori-shima mud volcano. This lowest velocity of 6.2 km/s corresponds to the highest percentage of serpentinization, equal to 54%. Based on these velocity models and assuming the relationships between velocity, density,

F4. Shear velocity vs. compressional velocity, p. 10.
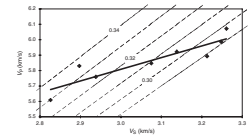
and serpentinization from Christensen (1966) apply, the most altered rock in the forearc wedge is closest to the subducting slab and to the Tori-shima serpentine mud volcano. We also note that the average calculated percent serpentine of the Leg 195 clasts (66%) is more than that determined from the seismic velocity model (maximum = 54%). It is likely that these clasts were either taken from zones of increased serpentinization at depth or experienced additional serpentinization after the clasts were removed from their host rock.

The relationship between velocity and density might also aid in the interpretation of gravity measurements over the trench axis. Using the seismic model and the velocity-density curves, densities could be assigned to the altered forearc wedge that could provide an additional constraint to a gravity model of the subduction zone.

SUMMARY

The clasts recovered from the South Chamorro serpentine mud volcano during Leg 195 have very narrow density and velocity ranges and a low microcrack content. The velocity-density relationships exhibit the linear trend established by Christensen (1966). The densities, velocities, and Poisson's ratios of the rocks all suggest very high percentages of serpentinization in the rocks. A comparison of the degree of serpentinization in these clasts compared to the serpentinization calculated from the Izu-Bonin seismic study conducted in a setting similar to the South Chamorro Seamount shows that these clasts experienced more serpentinization than the forearc wedge. In general, these velocity and density measurements may be used in future seismic and gravity studies to help constrain the lithologies and serpentinization at these subduction zones.

ACKNOWLEDGMENTS

REFERENCES

Ballotti, D.M., Christensen, N.I., and Becker, K., 1992. Seismic properties of serpentinized peridotite from the Mariana forearc. *In* Fryer, P., Pearce, J.A., Stokking, L.B., et al., *Proc. ODP, Sci. Results,* 125: College Station, TX (Ocean Drilling Program), 581–584.

Birch, F., 1961. The velocity of compressional waves in rocks to 10 kilobars, 2. *J. Geophys. Res.,* 66:2199–2224.

Christensen, N.I., 1966. Elasticity of ultrabasic rocks. *J. Geophys. Res.,* 71:5921–5931.

Christensen, N.I., 1985. Measurements of dynamic properties of rocks at elevated temperatures and pressures. *In* Pincus, H.J., and Hoskins, E.R. (Eds.), *Measurements of Rock Properties at Elevated Pressures and Temperatures.* Spec. Tech. Publ.—ASTM, 869:93–107.

Christensen, N.I., 1996. Poisson's ratio and crustal seismology. *J. Geophys. Res.,* 101:3139–3156.

Christensen, N.I., and Shaw, G.H., 1970. Elasticity of mafic rocks from the Mid-Atlantic Ridge. *Geophys. J. R. Astron. Soc.,* 20:271–284.

Fryer, P., 1992. A synthesis of Leg 125 drilling of serpentine seamounts on the Mariana and Izu-Bonin forearcs. *In* Fryer, P., Pearce, J.A., Stokking, L.B., et al., *Proc. ODP, Sci. Results,* 125: College Station, TX (Ocean Drilling Program), 593–614.

Fryer, P., 1996. Evolution of the Mariana convergent plate margin system. *Rev. Geophys.,* 34:89–125.

Fryer, P., Lockwood, J.P., Becker, N., Phipps, S., and Todd, C.S., 2000. Significance of serpentine mud volcanism in convergent margins. *Spec. Pap.—Geol. Soc. Am.,* 349:35–51.

Kamimura, A., Kasahara, J., Shinohara, M., Hino, R., Shiobara, H., Fujie, G., and Kanazawa, T., 2002. Crustal structure study at the Izu-Bonin subduction zone around 31°N: implications of serpentinized materials along the subduction plate boundary. *Phys. Earth Planet. Inter.,* 132:105–129.

Shipboard Scientific Party, 2002. Site 1200. *In* Salisbury, M.H., Shinohara, M., Richter, C., et al., *Proc. ODP, Init. Repts.,* 195 [Online]. Available from World Wide Web: **http://www-odp.tamu.edu/publications/195_IR/chap_03/chap_03.htm**. [Cited 2003-07-13].

Wepfer, W.W., and Christensen, N.I., 1988. Characterizing microcracks via a velocity–pressure relation. *Eos, Trans Am. Geophys. Union,* 68:1503.

Figure F1. Typical data plot of confining pressure vs. compressional velocity for Sample 195-1200A-6R-2, 54 cm. Curve fit is from Wepfer and Christensen (1988). Inset = acquired waveform at 600 MPa for the sample.
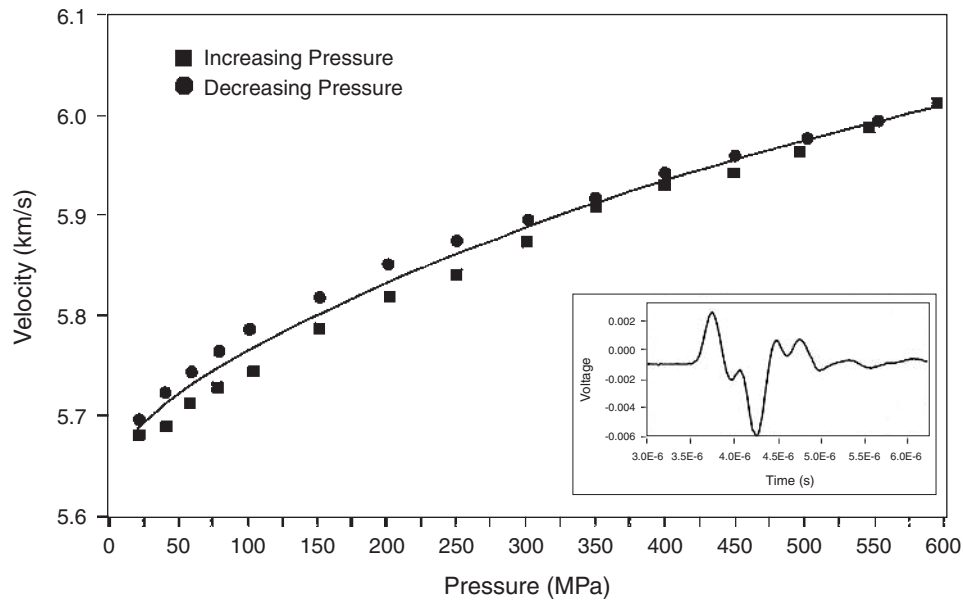
Figure F2. Confining pressure vs. average compressional velocity. Dashed lines = standard deviation.
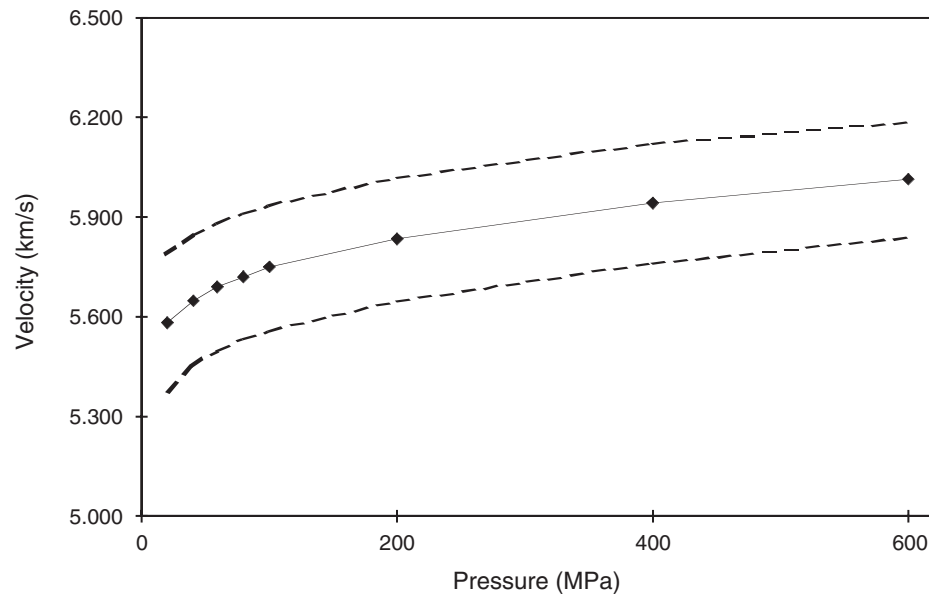
Figure F3. Compressional and shear velocities as a function of density at 200 MPa. Solid diamonds = Leg 195 samples; open diamonds = samples from Christensen (1966).

Figure F4. Shear velocity vs. compressional velocity at 200 MPa. Solid trend line through the data = least-squares solution. Solution $= 0.757x + 3.5375$. Dashed lines = constant Poisson's ratio.

Table T1. Density and compressional and shear velocities for Leg 195 serpentinites.

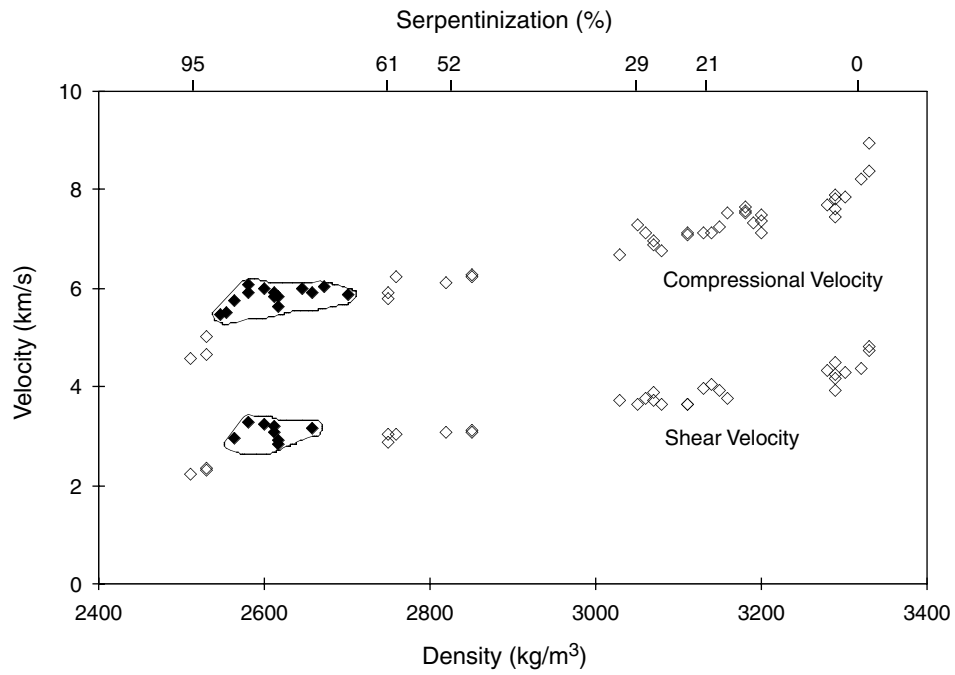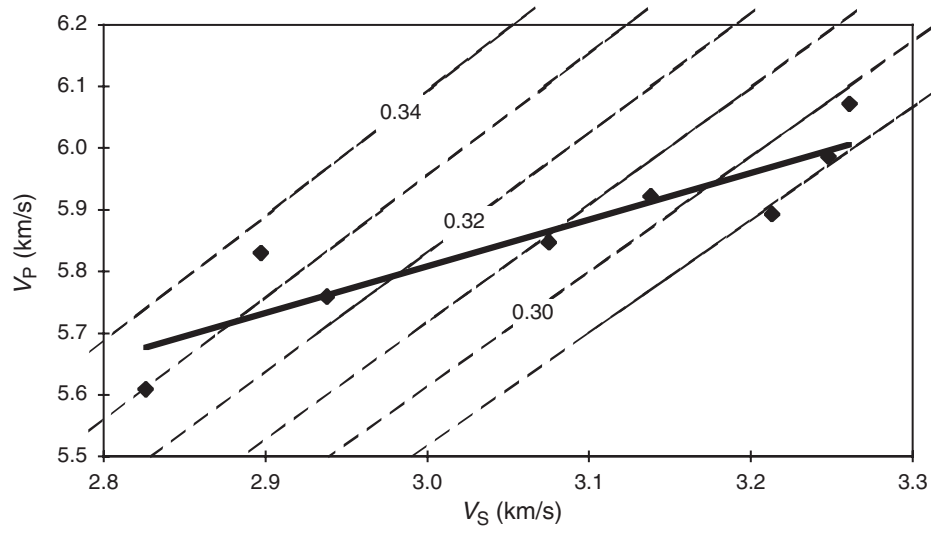| Core, section, interval (cm)	Depth (mbsf)	Density (kg/m^3)	Mode	Velocity (km/s)							
				20 MPa	40 MPa	60 MPa	80 MPa	100 MPa	200 MPa	400 MPa	600 MPa
195-1200A-											
3R-1, 17–19	18.37	2600	P	5.794	5.837	5.868	5.892	5.912	5.986	6.079	6.144
		2600	S	3.154	3.181	3.199	3.212	3.222	3.248	3.268	3.279
3R-1, 54–56	18.74	2580	P	5.784	5.878	5.931	5.967	5.994	6.072	6.140	6.180
		2580	S	3.167	3.184	3.199	3.213	3.224	3.261	3.285	3.288
6R-1, 104–106	42.44	2616	P	5.360	5.423	5.463	5.494	5.519	5.609	5.716	5.784
		2616	S	2.144	2.638	2.756	2.789	2.801	2.826	2.857	2.880
6R-2, 11–13	42.77	2611	P	5.680	5.720	5.746	5.766	5.783	5.847	5.942	6.025
		2611	S	3.013	3.030	3.040	3.048	3.054	3.075	3.100	3.117
6R-2, 32–34	42.98	2565	P	5.465	5.552	5.604	5.640	5.669	5.759	5.851	5.905
		2565	S	2.852	2.878	2.893	2.904	2.912	2.938	2.964	2.980
6R-2, 54–56	43.2	2618	P	5.686	5.710	5.730	5.747	5.763	5.830	5.931	6.004
		2618	S	2.758	2.791	2.812	2.829	2.844	2.897	2.964	3.008
7R-1, 25–27	51.35	2657	P	5.773	5.795	5.815	5.833	5.850	5.922	6.028	6.099
		2657	S	3.049	3.075	3.090	3.101	3.110	3.138	3.166	3.183
7R-2, 9–11	51.78	2701	P	5.520	5.627	5.691	5.737	5.773	5.886	6.001	6.069
7R-2, 89–91	52.58	2580	P	5.428	5.577	5.661	5.719	5.763	5.894	6.019	6.088
7R-2, 114–116	52.83	2645	P	5.716	5.791	5.837	5.871	5.899	5.992	6.102	6.177
12R-1, 20–22	99.2	2672	P	5.751	5.816	5.859	5.892	5.920	6.020	6.148	6.227
13R-1, 46–48	109.16	2613	P	5.708	5.767	5.793	5.810	5.825	5.893	6.003	6.078
		2613	S	3.161	3.175	3.183	3.190	3.195	3.213	3.235	3.252
16R-1, 76–78	138.36	2548	P	5.137	5.239	5.299	5.343	5.377	5.484	5.593	5.658
16R-1, 107–109	138.67	2554	P	5.316	5.347	5.373	5.395	5.416	5.503	5.638	5.750
Average		2612	P	5.563	5.634	5.677	5.709	5.735	5.824	5.932	6.003
Average		2609	S	2.878	2.967	2.996	3.011	3.020	3.050	3.082	3.101

Note: P = compressional, S = shear.

Table T2. Apparent V_P/V_S and Poisson's ratios for Leg 195 serpentinites.

Core, section, interval (cm)	Pressure (MPa)									
	40		100		200		400		600	
	V_P/V_S	σ	V_P/V_S	σ	V_P/V_S	σ	V_P/V_S	σ	V_P/V_S	σ
195-1200A-										
3R-1, 17–19	1.835	0.289	1.835	0.289	1.843	0.291	1.860	0.297	1.874	0.301
3R-1, 54–56	1.846	0.292	1.859	0.296	1.862	0.297	1.869	0.299	1.880	0.303
6R-1, 104–106	2.500	0.405	1.970	0.327	1.985	0.330	2.001	0.333	2.008	0.335
6R-2, 11–13	1.885	0.304	1.894	0.307	1.901	0.309	1.917	0.313	1.933	0.317
6R-2, 32–34	1.916	0.313	1.947	0.321	1.960	0.324	1.974	0.327	1.982	0.329
6R-2, 54–56	2.062	0.346	2.026	0.339	2.012	0.336	2.001	0.334	1.996	0.332
7R-1, 25–27	1.893	0.307	1.881	0.303	1.887	0.305	1.904	0.310	1.916	0.313
13R-1, 46–48	1.806	0.279	1.823	0.285	1.834	0.288	1.856	0.295	1.869	0.299
Average	1.968	0.317	1.904	0.308	1.911	0.310	1.923	0.314	1.932	0.316